INVESTIGATION OF METAL ION MOBILITY UNDER EXPOSURE TO DEACTIVATING AGENTS

Ryan Zelinsky
Advisor: Dr. William S. Epling
University of Virginia

Abstract

The interest in metal loaded zeolites as solid-state hydrocarbon storage materials has driven research focused on understanding the chemical environment of metallic active centers under exposure to various external conditions. Here, we synthesized Pd loaded zeolites with different Si/Al ratios. These samples were exposed to H_2O and CO containing streams at high temperature to test their durability after exposure to extreme environments. After the high temperature deactivation treatments, ethylene storage degraded. Further, NO_x storage improved after the aging treatments. Analysis by x-ray absorption spectroscopy (XAS) suggested that the Pd remained in the form of highly dispersed ionic Pd^{2+} before and after aging. Finally, Ag/BEA and Fe/BEA samples were prepared and evaluated against Pd/BEA as a potentially cheaper alternative. Ag/BEA showed promising preliminary results as a hydrocarbon storage material, and proved to be more durable after several hydrocarbon storage cycles than the original Pd/BEA hydrocarbon storage material.

Introduction

Metal loaded zeolite catalysts have been the subject of study for many useful applications. They are used as catalysts for hydrocarbon cracking[1], hydrocarbon oligomerization[2], methane coupling[3], methane oxidation[4], and many other applications.

Interest in zeolites as hydrocarbon storage materials has increased as of late in the automotive aftertreatment field, as low temperature hydrocarbon emissions continue to pose many problems to automobile manufacturers. Specifically, the cold-start phase of vehicle operation can contribute up to 60-80% of the total hydrocarbon emissions for current combustion technologies.[5,6]

Zeolites are often chosen as the support material for hydrocarbon storage due to their properties as solid acids and as molecular sieves.[7–10] Without an active catalytic metal, zeolites are unable to adsorb hydrocarbons in the presence of water, so metals are often added to the zeolite by ion-exchange.[11–13] Recent studies have highlighted zeolites exchanged with Ag[14–16] and Pd[17–22] as potential candidates for low temperature hydrocarbon traps. Zeolites with Pd ion-exchanged are currently the subject of study for many applications, including methane oxidation[23,24], Wacker oxidation[25,26], and as passive NO_x adsorbers (PNA)[27–32].

While Pd/Zeolites have been heralded as promising materials for the hydrocarbon storage application, the deactivation of these materials under realistic conditions has not been thoroughly studied. One method of simulated deactivation is by hydrothermal aging (HTA), which mimics real world degradation by accelerated means. HTA can be used to quickly simulate degradation and the materials can be characterized by their storage ability and by many other means.

While Pd/BEA has shown promise as a hydrocarbon trap material, Pd is a costly metal and may prove infeasible as the storage site for hydrocarbons in many applications. Alternative metals such as Ag[14,15], Cu[33], Pt[33], and Fe[34] have also been studied for potential use in hydrocarbon traps. These materials can also be studied, especially under exposure to deactivating agents. They can then be evaluated in comparison to the Pd/BEA baseline material.

In this work, we first investigate how high temperature exposure to deactivating agents such as CO and H_2O affects the Pd speciation in a Pd/BEA hydrocarbon trap. Reactor studies are used to test the ethylene storage capacity before and after aging. NO adsorption and TPD are used to probe differences in Pd speciation. X-ray absorption spectroscopy (XAS) is used to evaluate the chemical environment of the Pd before and after aging.

In addition to the work on Pd/BEA, we then also investigated Ag/BEA and Fe/BEA as potential cheaper alternatives to Pd/BEA for hydrocarbon storage. Cycling experiments were performed over the two best performing catalysts, Pd/BEA and Ag/BEA, to investigate the longevity of these materials after repeated use as hydrocarbon storage materials.

Experimental

Catalyst Synthesis

In this study, zeolite beta in the ammonium cation form, NH_4^+/BEA, was purchased from two vendors (Zeolyst and ACS Material). The powder was treated at 500°C in air for 4 hours to obtain the H^+ form, denoted H/BEA. To obtain Pd/BEA, a palladium precursor salt ($Pd(NO_3)_2$, Sigma Aldrich) was dissolved in 28% aqueous ammonia and added to the dry catalyst powder to form a slurry. The slurry was mixed vigorously with a glass rod for 10 minutes. The slurry was first dried at 120 °C in air for 2 hours. Then, the dry powder was transferred to a ceramic crucible and treated at 600 °C in air for 4 hours.

Ag/BEA was prepared by ion-exchange with an Ag/NO_3 solution, following a method adapted from Kyriakidou et al.[14] Fe/BEA was prepared by wetness impregnation with $Fe(NO_3)_3$ dissolved in nitric acid, following a method adapted from Boroń et al.[35]

The catalyst powders were all sieved to obtain particles between 40-60 mesh (250-400 μm) and placed into a 0.25-inch ID quartz tube. The quartz tube was loaded into a Thermo Fisher Scientific Lindberg Blue Mini-Mite tube furnace with K-type thermocouples placed in either end. Aged catalysts were prepared by exposing the Pd/BEA powder to 1000 ppm CO, 5% H_2O, 10% O_2, and balance N_2 for 24 h at 550, 600, or 650°C.

XAS

Pd K-edge (23450 eV) X-ray adsorption spectroscopy (XAS) was conducted over fresh and aged Pd/BEA samples at the 10-BM-B beamline at the Advanced Photon Source (APS) at Argonne National Laboratory. The catalyst was packed into a stainless-steel sample holder containing six wells. The sample holder was placed into a 1-inch ID quartz tube and sealed within an air-tight cell with valves allowing for gas flow. The samples were pretreated at 600 °C in 10% O_2/He for 1 h, then cooled to 80 °C. The tube was transferred to the beamline and exposed to reaction conditions, where in-situ XAS measurements were taken. The data were normalized and the edge energy was calibrated from the Pd foil in Athena software from the Demeter XAS analysis package. EXAFS spectra were fit, and parameters calculated, in the program Artemis of the same software package.

Reactor Tests

To measure the gas concentrations, an MKS 2030 series Fourier transform infrared spectrometer (FTIR) was attached downstream of the catalyst and bypass. Table 1 gives the gas concentrations used in this study.

Table 1. Feed gas concentration for each species.

Species	*Concentration*
N_2	Balance
O_2	10%
H_2O	5%
CO	500 ppm
C_2H_4	200 ppm
NO	200 ppm

The gas mixture was made from gas cylinders supplied by Praxair and controlled by MKS Instruments mass flow controllers. Water was supplied to the gas phase using a Bronkhorst controlled evaporator mixer. The space velocity was 50,000 hr^{-1} for all experiments and aging treatments, calculated assuming the flow conditions of a monolith. Simulated gas feed concentrations were verified through a bypass line before being introduced to the catalyst.

Each hydrocarbon and NO_x trapping experiment began with a pretreatment in 10% O_2/N_2 at 600 °C for 1 h to oxidize any residual carbon and establish a normalized starting point for each experiment. Next, the catalyst was cooled to 80 °C in 10% O_2/N_2 while the reactant gas mixture was established in the bypass. Once 80 °C was reached and unchanging, the reactant gas mixture was switched to the reactor, and the catalyst was exposed for to it 30 minutes. Then, during the subsequent temperature programmed desorption (TPD), the temperature was ramped from 80-600 °C at a rate of 20 °C/min. Ethylene uptake was calculated with data from the adsorption phase because ethylene desorbed partially as combustion products (CO and CO_2). NO_x uptake was calculated from the desorption phase as all NO_x desorbed as NO or NO_2.

Results and Discussion

Ethylene Adsorption

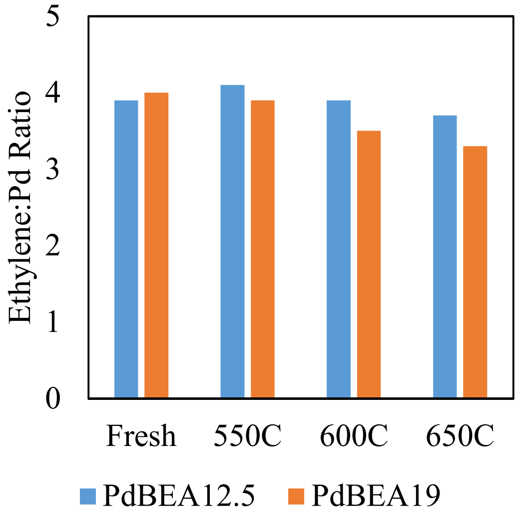

Figure 1: Ethylene adsorption over 0.5PdBEA19 and 0.5PdBEA12.5 before and after aging.

Ethylene adsorption experiments were performed to evaluate the hydrocarbon trapping efficacy of the fresh and aged catalysts. The results are shown in Figure 1. Ethylene uptake for each sample shows a decline in adsorption capacity as the aging severity increases. This trend held for Pd/BEA catalysts of each Si/Al ratio. In the presence of water, ethylene uptake will occur mainly on Pd sites, as it is known that water will competitively adsorb to the zeolite's Brönsted acid sites.[36] The loss of ethylene uptake points to a loss in active Pd sites. One explanation for this loss is the reduction and subsequent agglomeration of Pd during HTA.

NO Adsorption and TPD

One method to probe the dispersion of Pd cations is by NO adsorption, as atomically dispersed Pd^{n+} (n=1,2) is widely regarded as the active site in Pd/zeolite PNAs.[27,28,30,37–41] We exposed the catalysts to a stream of 200 ppm NO, 5% H_2O and 5% O_2 at 80 °C for 30 minutes, then performed a TPD in the presence of the same gas mixture while measuring the outlet NO_x concentration. The NO_x storage capacity increased with increasing aging severity for 0.5PdBEA12.5 (Table 2) and 0.5PdBEA19, and remained the same after aging for 0.5PdBEA75. The increase in NO_x storage capacity rules out a loss in ionic Pd, and rather points to an increase in Pd dispersion after aging.

Table 2. NO_x adsorption over Pd/BEA12.5

Pd/BEA12.5	*NO_x:Pd (Desorption)*
Fresh	0.42
Aged 550°C	0.52
Aged 600°C	0.58
Aged 650°C	0.60

Characterization by XAS

Another method to probe the chemical environment of the Pd in the fresh and aged catalysts is characterization by XAS. XAS measurements were carried out in He at 80°C on the fresh catalysts with all three Si/Al ratios, and the aged samples with Si/Al = 19. Data for Si/Al = 19 catalyst shown in Figure 2.

In the fresh catalysts, the Pd-O scattering path was fully coordinated, but the Pd-O-Pd path coordination varied between the three catalysts. The 0.5PdBEA75 sample had the highest Pd-O-Pd coordination, indicating a significant fraction of Pd exists as bulk PdO_x. The amount of exchanged Pd did not exceed the theoretical limit for ion exchange for this Si/Al ratio, but the existence of a relative lower concentration of Al^- sites may have played a role in its reduced dispersion. The Si/Al = 12.5 and 19 catalysts displayed a lower Pd-O-Pd coordination and thus only a smaller fraction of Pd existed at bulk PdO_x.

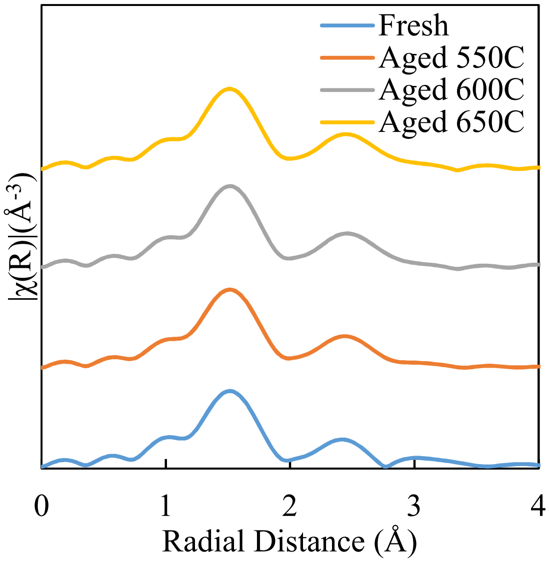

Figure 2: Fourier Transform of the EXAFS spectra for Pd/BEA19 over the Pd K-edge. Measurements taken at 80°C in He.

In the aged 0.5Pd/BEA19 samples, the Pd-O-Pd scattering path was insignificant for all three aging temperatures, indicating that HTA under these conditions did not promote the formation of bulk PdO_x, and rather, the aging may have even slightly promoted Pd dispersion as suggested above by the NO_x storage results.

The results of the ethylene and NO_x adsorption studies, combined with characterization by XAS, allow us to conclude that the Pd remains in an ionic state before and after aging, however the local environment of the Pd has changed from one species to another. Further characterization is required to assign a specific Pd^{n+} cation to each state, and is outside the scope of this work.

Ag/BEA and Fe/BEA Ethylene Adsorption

Ethylene adsorption experiments were carried out over 1% Ag/BEA and 1% Fe/BEA samples to evaluate their efficacy as a low temperature hydrocarbon storage material. The results are shown in Table 3. Fe/BEA did not appear to be active in ethylene storage, while Ag/BEA showed promising results.

Table 3. Ethylene Uptake over 1% Ag/BEA and 1% Fe/BEA

Catalyst	***Ethylene Uptake (μmol)***
1% Ag/BEA	5.2
1% Fe/BEA	0.21

Due to the apparent inactivity of Fe/BEA, Ag/BEA was selected for further study and comparison to Pd/BEA.

Low Temperature CO Exposure and Cycling

In our previous work[18] we reported that a wet CO co-feed severely decreased the ethylene adsorption capacity of Pd/BEA hydrocarbon traps. Here, we tested the effect of a wet CO co-feed on the Ag/BEA hydrocarbon trap. The results, Figure 3, show that an Ag/BEA hydrocarbon trap is almost completely unaffected by a CO and H_2O co-feed. The adsorption curve completely overlapped the curve in the case of no CO co-feed, while in comparison, the Pd/BEA catalyst was deactivated completely.

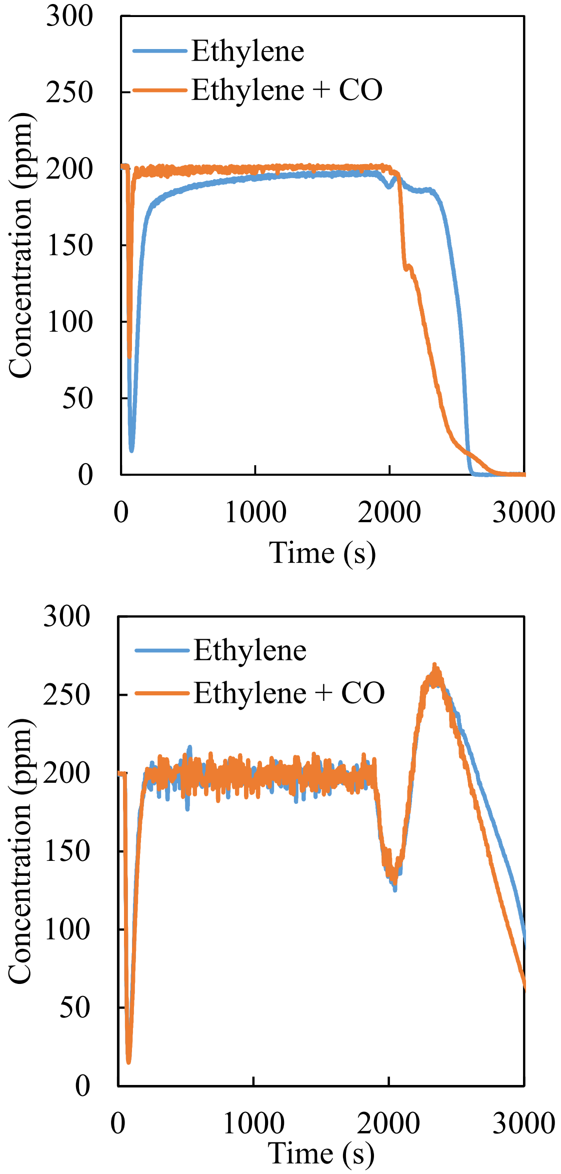

Figure 3: Ethylene concentration vs time during ethylene adsorption and TPD. Top: Pd/BEA. Bottom: Ag/BEA

In order to operate as a hydrocarbon storage material, the catalyst must also be able to sustain high activity after several cycles. The catalysts were exposed to reaction conditions in feeds containing both ethylene and CO, with inclusion of CO alternating from each cycle. Figure 4 shows the ethylene uptake curves after several cycles of exposure to both ethylene and CO.

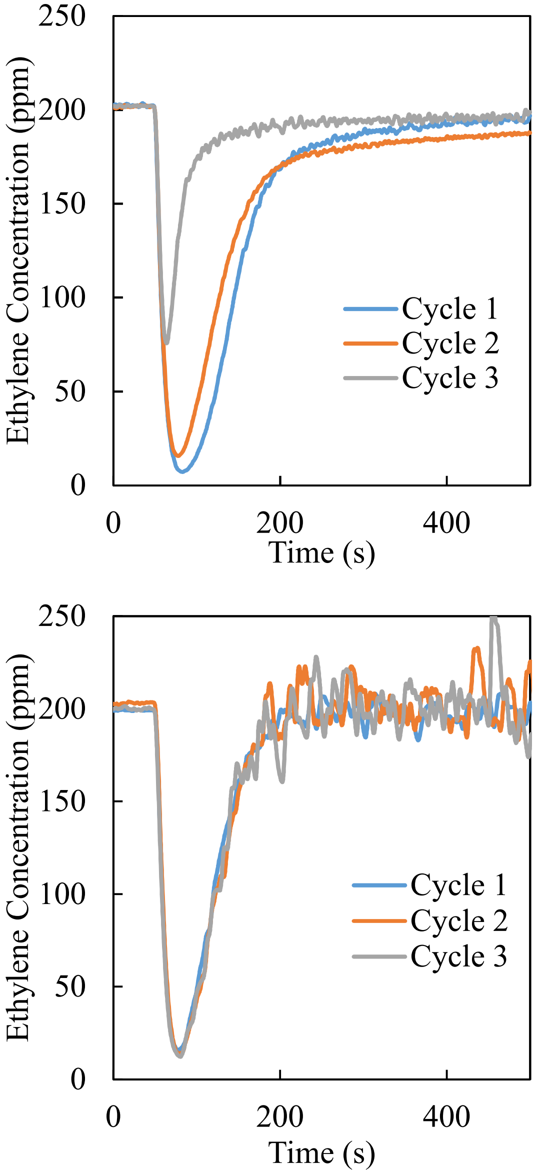

Figure 4: Ethylene uptake curves after exposure to ethylene and CO. Top: Pd/BEA. Bottom: Ag/BEA.

Repeated exposure to CO under the normal reaction conditions led to severe degradation of the Pd/BEA catalyst performance, while the Ag/BEA catalyst maintained high hydrocarbon trap capacity after 3 cycles of exposure to CO.

Conclusions

In this work, we conducted hydrocarbon trap experiments over Pd/BEA, Ag/BEA, and Fe/BEA samples. To simulate long term deactivation under reaction conditions, the Pd/BEA catalysts were subjected to high temperature exposure to CO and H_2O. The catalysts were characterized by ethylene and NO trapping experiments. Ethylene trapping efficiency declined after aging, while NO trapping increased after aging. The combination of these results suggested that ionic Pd transformed from one type of ionic species to another. This hypothesis was supported by characterization by XAS, which showed that the catalyst was fully ion-exchanged before and after aging.

Further testing of Ag/BEA and Fe/BEA was conducted to find a lower cost hydrocarbon storage catalyst. The Fe/BEA catalyst displayed very poor ethylene storage and proved to not be viable. The Ag/BEA catalyst showed promising ethylene storage and rivaled the performance of Pd/BEA. Further testing of the Ag/BEA catalyst under exposure to CO showed that this catalyst does not deactivate in the presence of CO. Cycling exposure to CO and H_2O did not deactivate the Ag/BEA catalyst, while the performance of the Pd/BEA catalyst dropped significantly after the third cycle. The results of these experiments show how low and high temperature exposure to deactivating agents can alter the chemical properties of metal loaded zeolites.

Acknowledgements

The authors would like to thank the Virginia Space Grant Consortium (VSGC) for funding this research for the academic year 2021-2022.

This research used resources of the Advanced Photon Source, a U.S. Department of Energy (DOE) Office of Science user facility operated for the DOE Office of Science by Argonne National Laboratory under Contract No. DE-AC02-06CH1135

References

1. Roldán, R. *et al.* Effect of the impregnation order on the nature of metal particles of bi-functional Pt/Pd-supported zeolite Beta materials and on their catalytic activity for the hydroisomerization of alkanes. *J. Catal.* **254**, 12–26 (2008).
2. Shephard, F. E., Rooney, J. J. & Kemball, C. *The polymerization of propylene on silica-alumina*. *Journal of Catalysis* vol. 1 (1962).
3. Borry, R. W., Kim, Y. H., Huffsmith, A., Reimer, J. A. & Iglesia, E. Structure and density of Mo and acid sites in Mo-exchanged H-ZSM5 catalysts for nonoxidative methane conversion. *J. Phys. Chem. B* **103**, 5787–5796 (1999).
4. Lou, Y. *et al.* Low-Temperature Methane Combustion over Pd/H-ZSM-5: Active Pd Sites with Specific Electronic Properties Modulated by Acidic Sites of H-ZSM-5. *ACS Catal.* **6**, 8127–8139 (2016).
5. Heck, R. M. & Farrauto, R. J. Automobile exhaust catalysts. *Appl. Catal. A Gen.* **221**, 443–457 (2001).
6. Hochmuth, J. K., Burk, P. L., Tolentino, C. & Mignano, M. J. Hydrocarbon traps for controlling cold start emissions. *SAE Tech. Pap.* 205–218 (1993) doi:10.4271/930739.
7. Heimrich, M. J., Smith, L. R. & Kitowski, J. Cold-start hydrocarbon collection for advanced exhaust emission control. *SAE Tech. Pap.* 1–12 (1992) doi:10.4271/920847.
8. Miano, F. Adsorption of hydrocarbon vapour mixtures onto zeolite 5A. *Colloids Surfaces A Physicochem. Eng. Asp.* **110**, 95–104 (1996).
9. Breck, D. W. *Zeolite molecular sieves: structure, chemistry, and use*. (1973).
10. Burke, N. R., Trimm, D. L. & Howe, R. F. The effect of silica:alumina ratio and hydrothermal ageing on the adsorption characteristics of BEA zeolites for cold start emission control. *Appl. Catal. B Environ.* **46**, 97–104 (2003).
11. Nunan, J., Lupescu, J., Denison, G., Ball, D. & Moser, D. HC traps for gasoline and ethanol applications. *SAE Tech. Pap.* **2**, 430–449 (2013).
12. Lupescu, J. A., Chanko, T. B., Richert, J. F. & Devries, J. E. Treatment of vehicle emissions from the combustion of E85 and Gasoline with catalyzed hydrocarbon traps. *SAE Tech. Pap.* 485–496 (2009) doi:10.4271/2009-01-1080.
13. Liu, X., Lampert, J. K., Arendarskiia, D. A. & Farrauto, R. J. FT-IR spectroscopic studies of hydrocarbon trapping in Ag+-ZSM-5 for gasoline engines under cold-start conditions. *Appl. Catal. B Environ.* **35**, 125–136 (2001).

14. Kyriakidou, E. A., Lee, J., Choi, J. S., Lance, M. & Toops, T. J. A comparative study of silver- and palladium-exchanged zeolites in propylene and nitrogen oxide adsorption and desorption for cold-start applications. *Catal. Today* (2020) doi:10.1016/j.cattod.2020.05.019.

15. Horvatits, C., Li, D., Dupuis, M., Kyriakidou, E. A. & Walker, E. A. Ethylene and Water Co-Adsorption on Ag/SSZ-13 Zeolites: A Theoretical Study. *J. Phys. Chem. C* **124**, 7295–7306 (2020).

16. Kang, S. B., Kalamaras, C., Balakotaiah, V. & Epling, W. Hydrocarbon Trapping over Ag-Beta Zeolite for Cold-Start Emission Control. *Catal. Letters* **147**, 1355–1362 (2017).

17. Zelinsky, R. & Epling, W. Effects of Multicomponent Hydrocarbon Feed on Hydrocarbon Adsorption–Desorption and Oxidation Light-Off Behavior on a Pd/BEA Hydrocarbon Trap. *Catal. Letters* **149**, 3194–3202 (2019).

18. Zelinsky, R. & Epling, W. S. Effects of co and h2o co-feed on the adsorption and oxidation properties of a pd/bea hydrocarbon trap. *Catalysts* **11**, 1–14 (2021).

19. Malamis, S. A., Harold, M. P. & Epling, W. S. Coupled NO and C3H6 Trapping, Release and Conversion on Pd/BEA: Evaluation of the Lean Hydrocarbon NOx Trap. *Ind. Eng. Chem. Res.* **58**, 22912–22923 (2019).

20. Lupescu, J. *et al.* A New Catalyzed HC Trap Technology that Enhances the Conversion of Gasoline Fuel Cold-Start Emissions. *SAE Int. J. Fuels Lubr.* **11**, (2018).

21. Xu, L. *et al.* Benefits of Pd Doped Zeolites for Cold Start HC/NOx Emission Reductions for Gasoline and E85 Fueled Vehicles. *SAE Int. J. Fuels Lubr.* **11**, 301–317 (2018).

22. Xu, L., Lupescu, J., Cavataio, G., Guo, K. & Jen, H. The Impacts of Pd in BEA Zeolite on Decreasing Cold-Start NMOG Emission of an E85 Fuel Vehicle. *SAE Int. J. Fuels Lubr.* **11**, 239–246 (2018).

23. Friberg, I. *et al.* Structure and performance of zeolite supported Pd for complete methane oxidation. *Catal. Today* **382**, 3–12 (2021).

24. Friberg, I., Sadokhina, N. & Olsson, L. The effect of Si/Al ratio of zeolite supported Pd for complete CH4 oxidation in the presence of water vapor and SO2. *Appl. Catal. B Environ.* **250**, 117–131 (2019).

25. Imbao, J., van Bokhoven, J. A., Clark, A. & Nachtegaal, M. Elucidating the mechanism of heterogeneous Wacker oxidation over Pd-Cu/zeolite Y by transient XAS. *Nat. Commun.* **11**, 1–9 (2020).

26. Imbao, J., Van Bokhoven, J. A. & Nachtegaal, M. Optimization of a heterogeneous Pd-Cu/zeolite y Wacker catalyst for ethylene oxidation. *Chem. Commun.* **56**, 1377–1380 (2020).

27. Mandal, K. *et al.* Condition-Dependent Pd Speciation and NO Adsorption in Pd/Zeolites. *ACS Catal.* **10**, 12801–12818 (2020).

28. Gu, Y., Sinha Majumdar, S., Pihl, J. A. & Epling, W. S. Investigation of NO adsorption and desorption phenomena on a Pd/ZSM-5 passive NOx adsorber. *Appl. Catal. B Environ.* **298**, 120561 (2021).

29. Gu, Y., Zelinsky, R. P., Chen, Y. R. & Epling, W. S. Investigation of an irreversible NOx storage degradation Mode on a Pd/BEA passive NOx adsorber. *Appl. Catal. B Environ.* **258**, 118032 (2019).

30. Mei, D., Gao, F., Szanyi, J. & Wang, Y. Mechanistic insight into the passive NOx adsorption in the highly dispersed Pd/HBEA zeolite. *Appl. Catal. A Gen.* **569**, 181–189 (2019).

31. Zheng, Y. *et al.* Low-Temperature Pd/Zeolite Passive NOx Adsorbers: Structure, Performance, and Adsorption Chemistry. *J. Phys. Chem. C* **121**, 15793–15803 (2017).

32. Chen, H. Y. *et al.* Low Temperature NO Storage of Zeolite Supported Pd for Low Temperature Diesel Engine Emission Control. *Catal. Letters* **146**, 1706–1711 (2016).

33. Westermann, A., Azambre, B., Finqueneisel, G., Da Costa, P. & Can, F. Evolution of unburnt hydrocarbons under 'cold-start' conditions from adsorption/desorption to conversion: On the screening of zeolitic materials. *Appl. Catal. B Environ.* **158–159**, 48–59 (2014).

34. Jonsson, R., Woo, J., Skoglundh, M. & Olsson, L. Zeolite beta doped with La, Fe, and Pd as a hydrocarbon trap. *Catalysts* **10**, 173 (2020).

35. Boroń, P. *et al.* Influence of iron state and acidity of zeolites on the catalytic activity of FeHBEA, FeHZSM-5 and FeHMOR in SCR of NO with NH3 and N2O decomposition. *Microporous Mesoporous Mater.* **203**, 73–85 (2015).

36. Park, J. H. *et al.* Promising zeolite-type hydrocarbon trap catalyst by a knowledge-based combinatorial approach. *Microporous Mesoporous Mater.* **117**, 178–184 (2009).

37. Villamaina, R. *et al.* Mechanistic insight in NO trapping on Pd/Chabazite systems for the low-temperature NOx removal from Diesel exhausts. *Appl. Catal. B Environ.* **284**, 119724 (2021).

38. Khivantsev, K. *et al.* Palladium/Beta zeolite passive NOx adsorbers (PNA): Clarification of PNA chemistry and the effects of CO and zeolite crystallite size on PNA performance. *Appl. Catal. A Gen.* **569**, 141–148 (2019).

39. Khivantsev, K. *et al.* Palladium/Zeolite Low Temperature Passive NOx Adsorbers (PNA): Structure-Adsorption Property Relationships for Hydrothermally Aged PNA Materials. *Emiss. Control Sci. Technol.* **6**, 126–138 (2020).

40. Ambast, M., Karinshak, K., Rahman, B. M. M., Grabow, L. C. & Harold, M. P. Passive NOx adsorption on Pd/H-ZSM-5: Experiments and modeling. *Appl. Catal. B Environ.* **269**, 118802 (2020).

41. Kim, P. *et al.* Investigation of the modes of NO adsorption in Pd/H-CHA. *Appl. Catal. B Environ.* **304**, 120992 (2022).